J Solid State Electrochem (2012) 16:847–855
DOI 10.1007/s10008-012-1643-5

ORIGINAL PAPER

Development of nonflammable lithium ion battery using a new all-solid polymer electrolyte

M. Wakihara · Y. Kadoma · N. Kumagai · H. Mita · R. Araki · K. Ozawa · Y. Ozawa

Received: 11 November 2011 / Revised: 17 December 2011 / Accepted: 2 January 2012 / Published online: 18 January 2012

Abstract For solving the safety issue of lithium ion batteries, the choice of all-solid polymer electrolyte is one of the possible solutions. However, usual polyethylene oxide including lithium supporting agent has not enough lithium ion conductivity as electrolyte for practical use. Some of our research group (M. W. and H. M.) have tried the addition of plasticizer such as borate ester or aluminate ester (Al-PEG) into monomer mixture containing lithium salt for increasing the ionic conductivity resulting in polymer electrolyte after polymerization. For such all-solid polymer electrolyte (SPE), the ionic conductivity, a value of 10^{-3} S/cm has been attained at 60 °C and the value will be acceptable for practical use. Since the SPE also has nonflammable property, the combination of the SPE with suitable cathode and anode may produce a new all-solid polymer battery with safety. In the present study, the SPE containing Al-PEG and dimethoxy ethylene glycol mixture as the plasticizer was newly combined with spinel $Li_4Ti_5O_{12}$ anode and olivine $LiFePO_4$ cathode objecting for developing stationary battery. The cell performance of the new combination will be reported at 30 °C and 50 °C.

Keywords All-solid polymer electrolyte · Aluminum ester plasticizer · Lithium ion batteries · Electrochemical performance

Contribution to the symposium: "The Origin, Development, and Future of the Lithium-Ion Battery", University of Texas at Austin, October 22, 2011

M. Wakihara (✉)
Tokyo Institute of Technology,
Oookayama,
Meguro-ku, Tokyo 152-8550, Japan
e-mail: mwakihar@k03.itscom.net

Y. Kadoma · N. Kumagai
Graduate School of Engineering, Iwate University,
4-3-5 Ueda-cho,
Morioka city, Iwate ken 020-8551, Japan

H. Mita · R. Araki
Nippon Nyukazai Co., LTD. 1-1 Chidori-cho,
Kawasaki ku,
Kawasaki city 210-0865, Japan

K. Ozawa · Y. Ozawa
Enax, INC., Colonnade Kasuga,
2-12-12 Kasuga,
Bunkyo-ku, Tokyo 112-0003, Japan

Introduction

The rechargeable lithium ion battery has crucial demands of our modern society, such as power source of various portable devices, and in the near future is expected for large-scale use, for example, as energy storage systems in mobile electric vehicle and in stationary day-to-night power shifts. However, conventional lithium ion batteries suffer from safety problems because they contain volatile and flammable organic solvents in the electrolyte solution. In order to improve the safety, alternative material systems for the electrolyte are urgently desired today. In this respect, there are many studies for developing (1) inorganic solid oxide electrolytes [1–4], (2) ionic liquid electrolytes [5, 6], and (3) poly(ethylene oxide) (PEO) by Wright et al. [7] and Armand et al. [8] at early stage. PEO and its derivatives have been known to be typically representative of the polymer matrix for the all-solid polymer electrolytes (SPEs). The PEO-based polymer dissolves lithium salt, i.e., the polymer plays the role of a solvent, since heteroatoms (oxygen atom, –O–) of polymer chains acting as electron donners coordinate lithium ions. Lithium ions are more likely to be coordinated by the heteroatoms on the same chain with the possibility of some coordination by neighboring atoms, and the chain must wrap around the lithium ion without excessive strain.

It is found that EO chain, $-(CH_2CH_2O)_n-$ provides just the right space for maximum solvation [9]. Molecular design of lithium salts with low lattice energy as well as matrix polymers is also important for obtaining higher ionic conductivity. Lithium bis-trifluoromethenesulfonimide (LiN $(CF_3SO_2)_2$, LiTFSI) with its low lattice energy (with high solubility) has been the most popular lithium salts from the time it was first reported by Armand et al. [10]. We thought that the selection of the PEO-based SPEs would be the fastest way for the realization of large-scale lithium ion battery with nonflammable property. The production cost also would be acceptable. However, since PEO-based SPEs have relatively low ionic conductivity (10^{-7} to 10^{-5} S cm^{-1}) at room temperature, we have tried to add tris(methoxy poly (ethylene glycol)) borate ester (B-PEG) [11–13], tris (methoxy poly(ethylene glycol)) aluminate ester (Al-PEG) [14] and dimethoxy ethylene glycol (DMTG) with a smaller viscosity value in monomer mixture as plasticizers before polymerization for increasing the lithium ion conductivity in PEO-based SPEs. It is also expected that a group of 13 elements in B-PEG and Al-PEG may work as Lewis acid and interact with counter anion of lithium salt in the monomer mixture which leads to the easier diffusion of lithium ion in the polymer electrolyte. Actually, the ionic conductivity in the PEO-based SPEs after polymerization has been successfully increased by the addition of B-PEG or Al-PEG and showed a value of 10^{-4} S cm^{-1} at 30 °C and 10^{-3} S cm^{-1} at 60 °C, while that in SPE without these plasticizers was less than 10^{-5} S cm^{-1} at 30 °C [11–14].

Usually in B-PEG, small amount of impurity in water remains along with the synthesis reaction (see Fig. 1a). The residual amount of water easily causes a hydrolysis reaction with the B-PEG plasticizer. In the present study, we mixed two kind of plasticizers, Al-PEG and dimethoxy ethylene glycol (see Fig. 1c), in the SPE. Basic electrochemical properties such as ionic conductivity, voltage window, transport number of lithium ion etc., of the PEO-based SPE already have been examined [14–16], and the viscosity of the monomer mixture before polymerization in the previous studies was higher than 130 mPa s. For easier penetration of the monomer mixture into the porous electrode, the viscosity was adjusted to about 75 mPa s by adding DMTG with a smaller viscosity to Al-PEG with a higher value as the plasticizer in the present study. The polymerization process of the monomer mixture was analyzed by DSC, and the electrochemical properties of the present SPE film showed almost similar behavior to the films in our previous studies [11–14]. Using the PEO-based SPE, a newly combined cell, $Li_4Ti_5O_{12}$(LTO)|PEO-based SPE containing Al-PEG + DMTG (=SPE)|$LiFePO_4$(LFP) has been constructed because both of LTO anode with spinel structure and LFP cathode with olivine structure accompany each stable phase change without serious heat evolution during lithium intercalation/deintercalation based on charge/discharge reactions. The electrochemical behavior of the cell will be reported at temperatures 30 °C and 50 °C.

Experimental

Preparation of PEO-based SPE films and cell make

The plasticizers, B-PEG and Al-PEG, were synthesized by the reaction of methoxy poly(ethylene glycol) $CH_3O(CH_2CH_2O)_nH$ and boric acid anhydride (B_2O_3) or aluminum isopropoxide at 100 °C under inert atmosphere as shown in Fig. 1a, b. DMTG with n=3 was supplied by Nippon Nyukazai Co. Ltd. Since the prepared liquid B-PEG simultaneously contains small amount of impurity water (Fig. 1a) which may lead to the cause of swelling of a laminate cell after cycling, we newly used a liquid mixture of Al-PEG with EO chain n=9 and DMTG with EO chain n=3 as the plasticizer in order to reduce the total viscosity of monomer mixture. The total viscosity was adjusted to about 75 mPa s in the present study by putting DMTG with a smaller viscosity, 3.8 mPa s to Al-PEG with a higher viscosity, >130 mPa s. However, the amount of added DMTG was almost limited to less than 15 wt.% of the total monomer weight for maintaining nonflammable property. The details of the preparation are described previously [11, 14]. The matrix for the polymer electrolytes was a copolymer of two types of poly(ethylene glycol) methacrylate, one was PEG-monomethacrylate (abbreviated to PME400 (MPG-130MA), Nippon Nyukazai Co. Ltd) and the other PEG-dimetacrylate (PDE600) (Fig. 1d, e), with a molar ratio of 5:1 (=PME400:PDE600). The mixture of plasticizers, Al-PEG (n=9) + DMTG (n=3), (Al-PEG/DMTG ratio=1.5 in weight), was mixed to the matrix component (PME400 + PDE600), in almost equal amounts in weight. LiTFSI (Fluka) was dissolved in the above solution to give a molar ratio of lithium and ethylene oxide (EO) units in polymer electrolyte of 1/20. Benzoyl peroxide (0.5% of monomer mixture in weight) was also added into the monomer mixture solution as an initiator for polymerization. The radical polymerization is usually carried out by heating or UV irradiation. In the present study, a heating system was chosen for the polymerization from the cost performance and easier manipulation. Before the polymerization, the monomer mixtures were painted on the cathode film (LFP/AB/binder=83:10:7 in weight and cathode thickness, about 50 μm, prepared by Enax Inc.) by controlling the thickness of the monomer under vacuum and then heated to about 120 °C followed by keeping for several hours to complete the polymerization. The two types of thickness of the polymer electrolyte film (SPE), about 25 and 50 μm were prepared. The combination of the SPE with LTO anode and LFP cathode was selected. The anode film (LTO/AB/

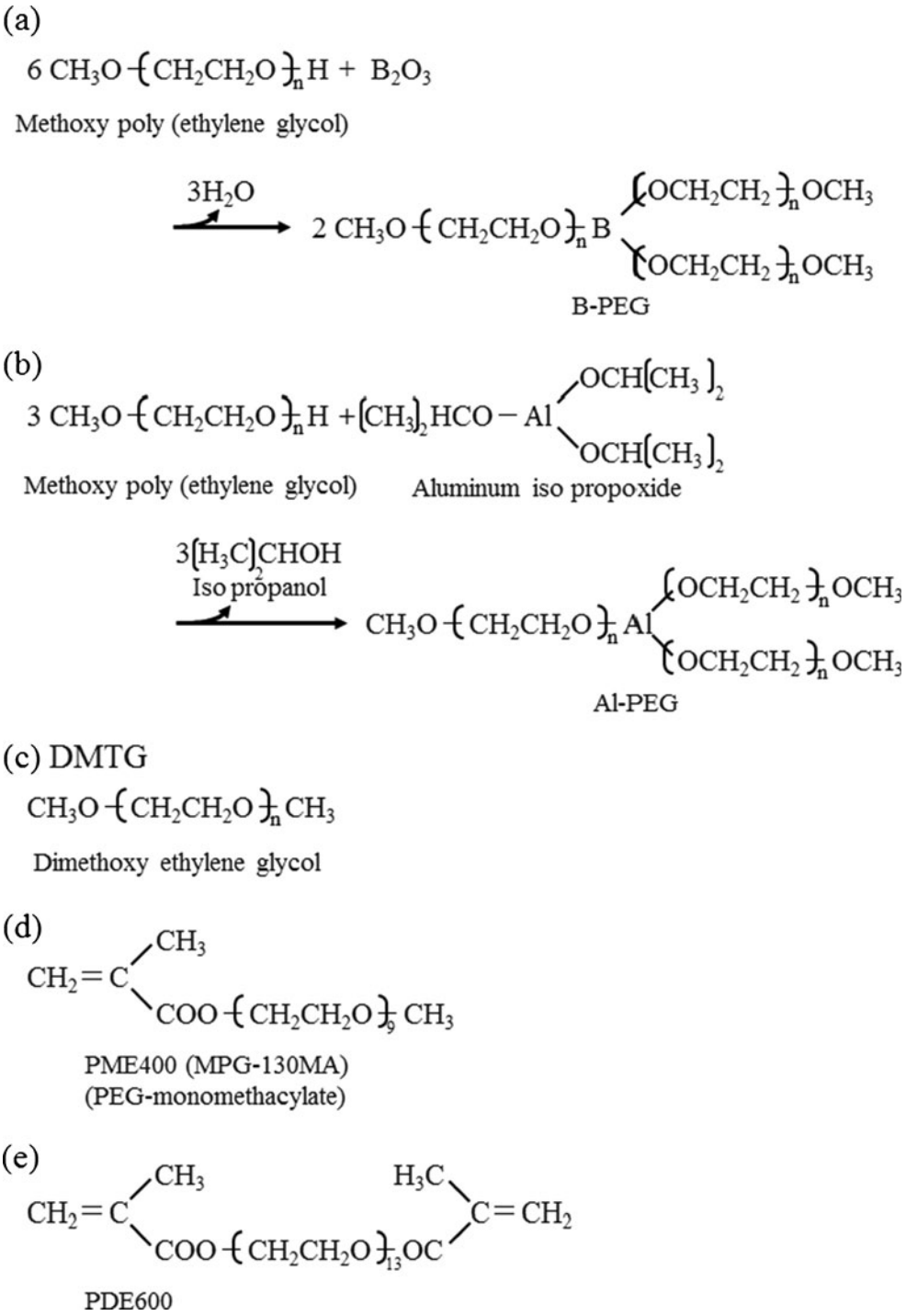

Fig. 1 Synthetic reaction of B-PEG (**a**) and Al-PEG (**b**). Molecular structure of DMTG (**c**), PME400 (**d**), and PDE600 (**e**)

binder=90:5:5 in weight; anode thickness, about 20 μm, prepared by Enax Co. Ltd) was set on the polymer film. Some of laminate-type single cell (68×68 mm) were assembled by using aluminum foil (thickness, 15 μm) for both electrodes under vacuum condition. The molar ratio of the anode/cathode active materials (A/C ratio) was set at 0.9 in the present study. The new laminate cell LTO|SPE|LFP was galvanostatically charge/discharged on the multichannel battery tester (Hokuto Denko, HDJ501 SM8A) between 1.7–2.05 V vs. Li^+/Li for 0.1 °C at temperatures 30 °C and 50 °C, respectively. The cross-section of the cell after the 50th cycle was observed by SEM photograph for evaluating the electrode/electrolyte interface after cycling.

Thermal and electrochemical studies and NMR measurement

Before assembling the cell, thermal behavior of the polymerization of the monomer and the electrochemical

properties of the prepared PEO-based SPE film were examined. The polymerization process of the monomer mixture was analyzed by DSC (Bruker AXS 3100SA) from a room temperature to about 120 °C at heating rate 10 °C/min under N_2 atmosphere putting a small amount of monomer mixture in a small aluminum-made sealed container with a very small hole in the top of the center part. CV measurement and AC impedance experiments besides NMR measurement were examined using similar techniques previously reported [11–17]. The SPE film (thickness, about 1 mm) was newly prepared for the measurements. CV measurement was carried out by using potentiostat/galvanostat (Bio-Logic VSP) in the voltage range 2–5 V with a sweep rate 1 mV/s using two electrode cell, Li|SPE|SUS (stainless uses steel, SUS304) at 30 °C and 50 °C [14]. The temperature dependence of the ionic conductivity of the SPE was determined through AC impedance experiments using a Hewllet-Packard 4192A LF impedance analyzer over the frequency range from 5 Hz to 13 MHz [17]. The ^{7}Li and ^{19}F NMR experiments were carried out using a Bruker Avance DSX 300 NMR spectrometer operating at 300.11 MHz for ^{1}H with a field-gradient generator system (PGStE-NMR) for estimating transport number of lithium in the SPE [16, 17]. The details of the PGStE-NMR method are described in our previous papers [16, 17]. For evaluating the effect of Lewis acidity of Al-PEG in the present SPE, the data of the previous NMR will be shown in this paper.

Results and discussion

Figure 2 shows the DSC curve of the polymerization of the monomer mixture in the present study. The heating was carried out from a room temperature to 120 °C at a heating rate of 10 °C/min. From the curve, it seems that the polymerization starts at about 80 °C and finishes after 12 min. The exothermic heat, 22.6 cal/g (=94.5 J/g) was evaluated from the curve although the baseline was deviated from the original line. Even so, the heating of the monomer mixture at 120 °C for several hours would be sufficient enough for complete polymerization. From the IR measurement (not shown) of the prepared SPE film, C=C double bond peak at 1,640–1,650 cm^{-1} disappeared. This also supports the complete polymerization.

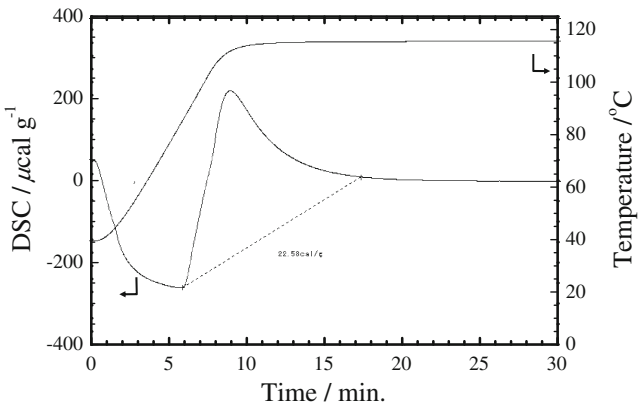

Fig. 2 DSC curve of polymerization of monomer mixture. Heating rate is 10 °C/min

Figure 3 shows the Arrhenius plot of the ionic conductivity of the SPE. Open symbols correspond to the conductivity of the SPE containing both Al-PEG + DMTG plasticizers, while solid symbols reveal that of SPE without any plasticizer. As can be seen, the addition of plasticizers in the SPE enhances the conductivity by about one order of magnitude and the conductivity value reached 10^{-3} S cm^{-1} at 60 °C. A value of $10^{-3.6}$ S cm^{-1} could be obtained even at room temperature. These values suggest the possibility of practical use of the SPE, if suitable thin film manipulation of the SPE is attainable. CV curves of the present SPE are shown in Fig. 4. Five cycles were carried out between 2.0–5.0 V vs. Li^{+}/Li at a scan rate, 1 mV/s, using two electrode cell, Li|SPE|SUS. The oxidation of the SPE seems to start over 4.3 V at room temperature (Fig. 4a), while at 50 °C it may begin at lower than 4.0 V or so on (Fig. 4b). In the reduction range, some of decomposition reaction of the SPE may proceed at lower than 3.0 V, although each extent for the cycle is tiny. The decomposition reaction gradually seems to accelerate at higher temperature. The voltage window of the SPE seems to be existing in the range between 4.0 and 3.0 V vs. Li^{+}/Li. From these curves, it is implied that one of the suitable combination of cathodes with the present SPE will be olivine-type $LiFePO_4$ (LFP), first proposed by Goodenough et al. [18], which has a flat discharge voltage at 3.4 V vs. Li^{+}/Li alternative to layered $LiCoO_2$ (space group *R*-3*m*) and cubic $LiMn_2O_4$ (space group *Fd*-3*m*) spinel with

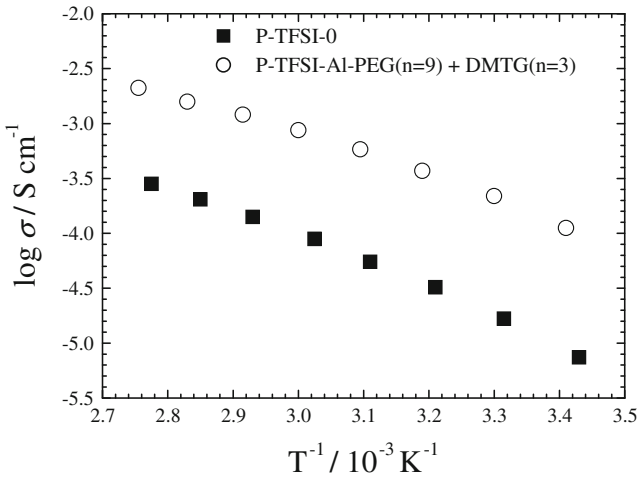

Fig. 3 Arrhenius plots of ionic conductivity. *Open symbols* correspond to the present SPE containing Al-PEG n=9 and DMTG n=11 plasticizer. *Solid symbols* mean the SPE without plasticizer

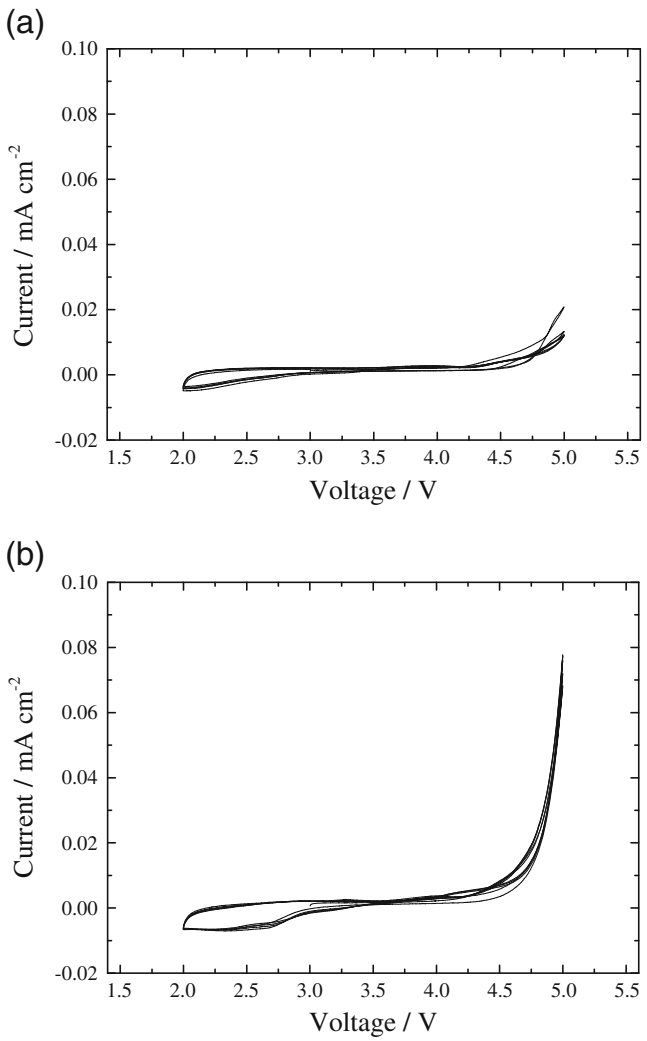

Fig. 4 CV measurement of the present SPE in the voltage range between 2.0 and 5.0 V vs. Li^+/Li at 30 °C (**a**) and 50 °C (**b**) at scan rate 1 mV/s

charge/discharge voltage higher than 4.0 V vs. Li^+/Li. In the present study, the LFP was selected for the cathode active material. From the ecological, safe, and economical point of view, the LFP (space group *Pnma*) also seems to be one of the most attractive candidates. In the LFP structure, small tetrahedral PO_4 is isolated and has strong covalency, while octahedrally coordinated lithium and iron ions show strong ionic character. This leads to a favorable high redox potential (~3.4 V) for Fe^{3+}/Fe^{2+} at the expense of low electronic conductivity (~10^{-9} S cm^{-1} at room temperature). However, the further efforts to increase its conductivity through intimate carbon coating have improved the early problem [19]. Usually lithium ion in the LFP diffuses one-dimensionally in the [010] direction channel with a curved trajectory between adjacent sites accompanying the phase change (LFP–$FePO_4$) [20, 21], and the theoretical energy capacity reaches about 170 mAh/g. The heat flow due to the insertion of lithium into the electrode material can be written [22, 23] as

$$p = -I\mathrm{T}(\Delta \mathrm{S})/\mathrm{n}F) - I\left(E_{\mathrm{eq}} - E_{\mathrm{i}}\right) = I\mathrm{T}(dE/d\mathrm{T}) - I\left(E_{\mathrm{eq}} - E_{\mathrm{i}}\right) \quad (1)$$

where p is heat flow, I is current, n is number of electron, F means the Faraday constant, E means open circuit voltage (OCV), E_{eq} and E_i correspond to electrode potential at equilibrium and at experimental state, respectively. In order to estimate the heat flow, charge/discharge experiment usually is carried out at very low current density. Accordingly, E_{eq} and E_i approximately are equal value. Therefore, Eq. 1 is approximated as follows,

$$p \fallingdotseq I\mathrm{T}(\Delta S)/nF) = I\mathrm{T}(dE/d\mathrm{T}) \quad (2)$$

From Eq. 2, no heat flow would be expected at the phase transformation range during charge/discharge reaction theoretically because dE/dT term draw a flat at the OCV curve which means zero. Miyashiro [24] actually measured the heat flow of LFP–$FePO_4$ phase transformation range by making use of modified Calvet-type of twin calorimeter (Tokyo Riko Co. Ltd) and recognized almost no heat flow effect during the phase change, LFP–$FePO_4$, accompanying lithium intercalation/deintercalation. This suggests that the LFP will be one of excellent candidates of the cathode for large-scale lithium ion batteries for lasting. These are main reasons why the LFP was used as the cathode in the present study.

PGStE-NMR measurements can give the diffusion coefficients of lithium- and fluorine-containing species separately. The diffusion attenuation of the spin-echo, from which the diffusion coefficient of the Li and F nuclei, D_{Li} and D_{F}, were estimated, is given by Eq. 3.

$$A(g) = A(0)\exp[-\gamma^2\delta^2 g^2 D(\Delta - \delta/3)] \quad (3)$$

The details related to Eq. 3 are described elsewhere [25]. However, the values of the diffusion coefficients obtained mean the total of charged and non-charged species such as dissolved ions and non-dissolved salt, i.e., the D_{Li} value in the present SPEs may contain simultaneous contribution both from the diffusion of dissolved Li^+ and associated LiTFSI molecules. The diffusion coefficients of D_{Li} and D_{F} of the polymer electrolyte containing B-PEG, Al-PEG, and/or DMTG as plasticizers and the transport numbers, t_{Li}, $t_{\mathrm{Li}}{}^+$, and t_{F} in the SPEs have been already measured in our research group for estimating the extent of the effect of Lewis acidity in the SPES [16, 17]. For estimating t_{Li}, the equation, $t_{\mathrm{Li}}=D_{\mathrm{Li}}/(D_{\mathrm{Li}} + D_{\mathrm{F}})$, presented by Watanabe et al. [26] was used. In the equation, they assumed a small interaction between the cation and the anion, such as in the condition of the dilute system for lithium salt concentration, and/or almost unity for the dissociation ratio. Using the

equation of t_{Li}, the Arrhenius plot of t_{Li} of the polymer electrolyte SPE containing Al-PEG and DMTG as plasticizers is shown at the temperature range between 40 °C and 70 °C in Fig. 5a. From the data of t_{Li}, it is seen that the diffusion of the anion part is less than the cation part suggesting no remarkable Lewis acidity of Al-PEG in the SPE, even if some of hypothesis are included in the equation of t_{Li}. We thought that some of interaction between Al and ether oxygen within the Al-PEG plasticizer may cause a self-neutralization of the Lewis acidity [17]. The diffusion coefficients D_{Li} and D_F obtained by PGStE-NMR can be linked to the molar conductivity Λ_{NMR} by the Nernst–Einstein equation. On the other hand, the molar conductivity obtained from the impedance measurements, Λ_{imp} is estimated by assuming that the dissociation ratio is nearly equal to unity. From the both Λ_{NMR} and Λ_{imp}, the apparent dissociation ratio, β, can be expressed by Eq. 4 [17, 26]

$$b = \Lambda_{imp}/\Lambda_{NMR} \tag{4}$$

The apparent dissociation values β in the SPE containing Al-PEG (n=9) are plotted in Fig. 5b. The precise discussion on the β values is not able to develop here because of the hypothesis in the Eq. 4, whatever the dissociation of LiTFSI in the SPE containing Al-PEG is less than that in the SPE

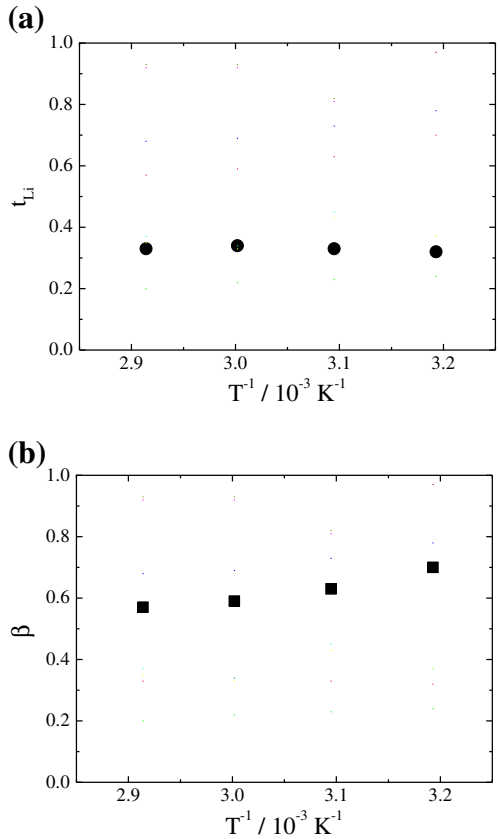

Fig. 5 t_{Li} values in the SPE (**a**) and the apparent dissociation ratio β of LiTFSI in the SPE (**b**) using equations in [26]

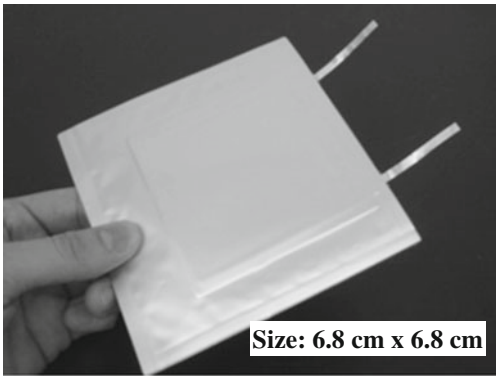

Fig. 6 Picture of laminate-type single cell in the present study. The size of the electrodes and the electrolyte is 68×68 mm

with B-PEG [17]. While the diffusion coefficient of the SPE with Al-PEG is higher than that with B-PEG [17]. Some indices are desirable for developing suitable nonflammable

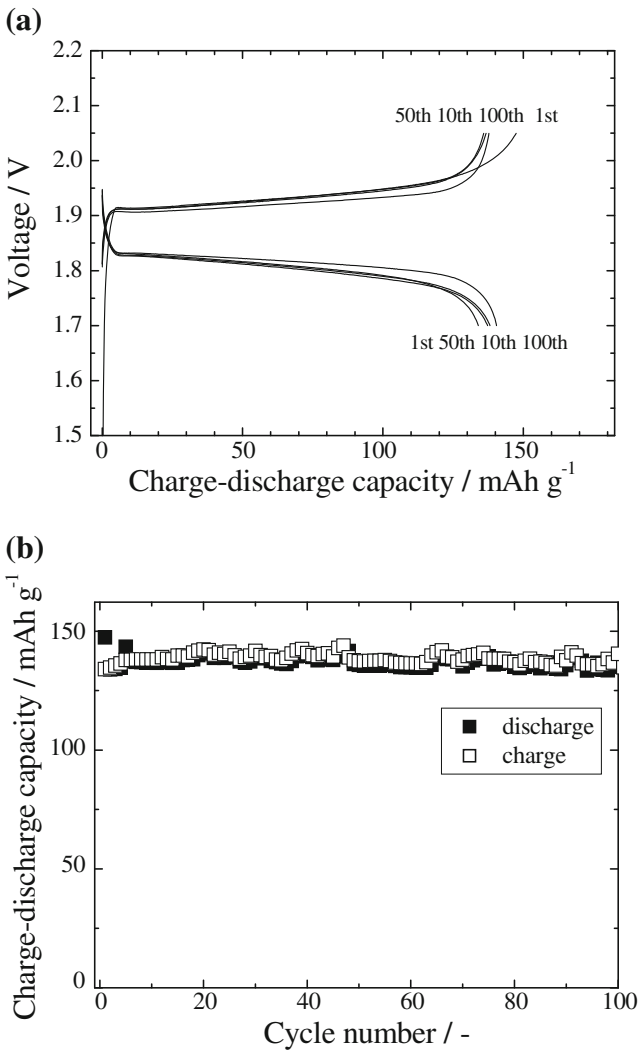

Fig. 7 Charge/discharge curves for cycling at 0.1 C (30 C) (**a**) and cycle performance of the cell up to the 100th cycle at 30 C (**b**)

safe SPEs with plasticizers. The development of new analytical equation of the transport numbers, t_{Li} and t_{Li}^{+}, considering the concentration of plasticizers also will be required for expanding more precise analysis on the behavior of lithium ion in the SPEs in the near future.

The combination of usual carbon anode with the SPE containing Al-PEG electrolyte never has given a long-life cycling performance as far as we are concerned. Accordingly, $Li_4Ti_5O_{12}$ (LTO, $Li[Li_{1/3}Ti_{5/3}]O_4$) with spinel structure (space group *Fd*-3*m*) was adopted for the anode in the present study. In the LTO structure, the lithium ions migrate from 8a tetrahedral sites to vacant 16c octahedral sites, like –8a–16c–8a–. The lithium insertion into the LTO accompanies the phase transformation to ordered rock-salt-type structure, $Li_2[Li_{1/3}Ti_{5/3}]O_4$ [27–31] without any remarkable volume change [30, 31], although it shows 1.5 V vs. Li^{+}/Li higher operation voltage than the graphite-negative electrode widely used in current lithium ion batteries. Ohzuku et al. [31] reported the lattice parameter change from LTO to $Li_2[Li_{1/3}Ti_{5/3}]O_4$ only from a=8.357 Å to a=8.356 Å. It is pointed out by many researchers [27–31] that such an almost zero-strain is an ideal electrode for long-life lithium ion batteries, even if the total cell voltage falls below around 2.5~1.8 V vs. Li^{+}/Li depending on the combination with the cathode material.

Figure 6 shows the photograph of a laminate-type single cell of LTO|SPE|LFP in the present study. The net size of the electrode and the electrolyte is 6.8×6.8 cm. We prepared two types of single cell in which the thickness of the electrolyte is 25 and 50 μm. Since the charge/discharge properties of both cells showed similar cyclic behavior, it seems that the rate determining step will exist in the electrode/electrolyte interface. The charge/discharge curves from the first to the 100th cycle operated at a current density of 0.1 C in voltage range of 1.7–2.05 V at 30 °C are shown in Fig. 7a and the cycling performance up to the 100th cycle is illustrated in Fig. 7b, respectively. The thickness of the polymer electrolyte in the cell was 50 μm. Although the polarization of the charge and the discharge seems to be relatively high, the cell shows rather smooth curves with average discharge voltage, 1.8 V vs. Li^{+}/Li and about 140 mhA/g of rechargeable capacity (cathode capacity). As can be seen in Fig. 7, coulombic efficiency is ca. 100% except for the irreversibility at the first several cycles. Sufficient penetration of monomer mixture into porous components in the cathode seems to be attained before the polymerization through such a higher capacity density. Figure 8 also shows the charge/discharge cycle performance under the current density, 0.1 C, at 50 °C. The polarization during the charge/discharge

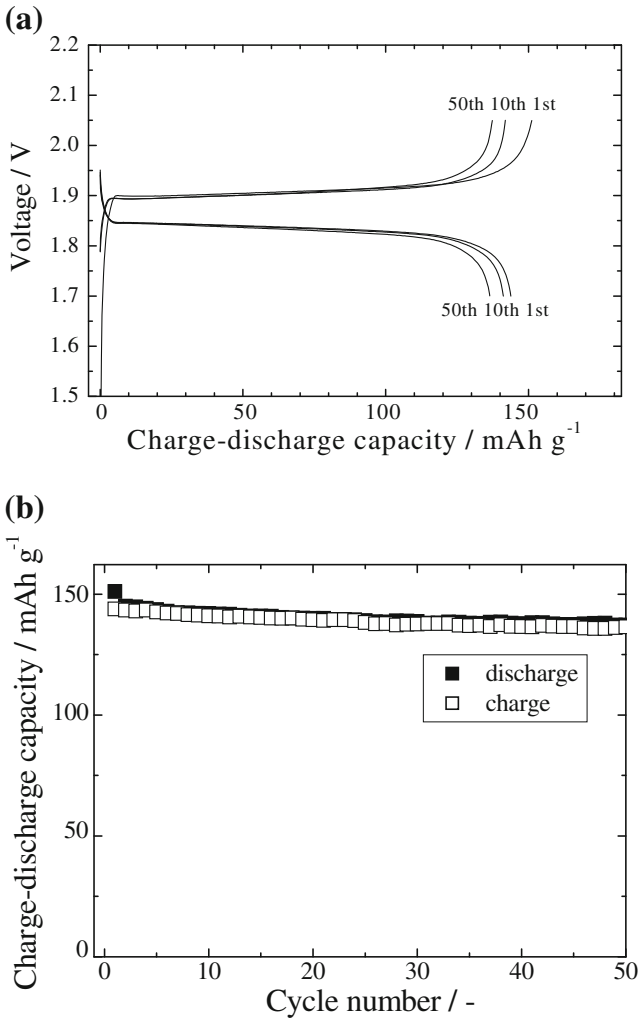

Fig. 8 Charge/discharge curves for cycling at 0.1 C (50 C) (**a**) and cycle performance of the cell up to the 50th cycle at 50 C (**b**)

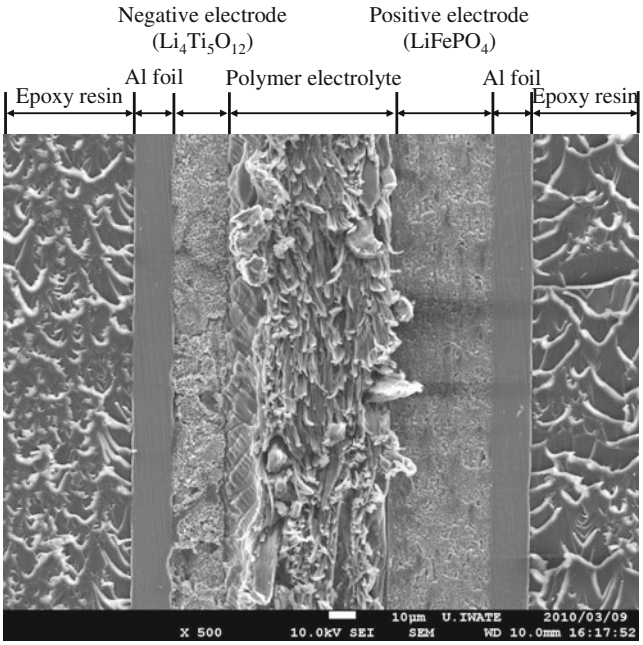

Fig. 9 Photograph of the cross-section of the present cell after 50th cycle

reaction decreased in comparison with that at 30 °C, and a higher average discharge voltage, about 1.83 V vs. Li^+/Li, was observed as shown in Fig. 8a. However, gradual capacity fade happened as the cycling proceeded (Fig. 8b). The decline of coulombic efficiency at each cycle was about 0.1% after the tenth cycle. For further understanding of the decay mechanism of the capacity retention, AC impedance measurements are useful and serve as a diagnostic tool for LPBs. In our previous studies [15, 16], the AC impedance of the cell, Li|SPE|LFP, was measured at the first cycle and after the 60th cycle. The charge transfer resistance at the cathode/polymer electrolyte interface increased after cycling. In order to observe the aspect of the interface, SEM/EDX analysis also was carried out. Actually, the amount of fluorine on the surface of the LFP cathode increased after cycling. The fluorine can be supplied only from lithium salt, LiTFSI, in the SPE, and some of TFSI ions may be decomposed on the surface of the LFP cathode [17] leading to the formation of SEI. From these facts and the assumption, the capacity fade at higher temperature may be caused by the accumulation of very thin SEI after cycling. To maintain stable capacity retention, suitable treatment on the surface of the LFP cathode will be necessary. The addition of inorganic compound, $AlPO_4$, to polymer electrolyte containing B-PEG as a plasticizer improved cycle performance of the cell in our previous study [32]. However, the chemistry of the electrode surface processes in lithium polymer batteries is not well understood because of thin nanolayer. A simple model of the surface modification considering the space charge was proposed in our previous study [15]. The surface modification may make an improved high-rate performance even if it covers only limited area on the surface of the cathode [32].

Figure 9 shows the photograph of cross-section of the present single cell after the 50th cycle. The thickness of the polymer electrolyte is 50 μm. Epoxy resin in both sides in the photo works as supporter of the cell for taking the SEM photograph. Even after the 50th cycle, the present SPE seems to maintain stable feature working also as separator besides the conductor of lithium ions. Al foil current collector of both the cathode and the anode almost kept the original state. According to the literature [33], it is reported that LiTFSI in electrolyte causes Al foil corrosion at higher voltage. However, no such corrosion was seen from the SEM observation (Fig. 9). It is also reported that CV curve for Li|SPE|Al foil did not show any anodic current even at >3.85 V vs. Li^+/Li after cycled at 60 °C [34]. Hence, we can disregard anodic corrosion in the present cell.

For evaluating the safety of the present cell, nail test and overcharge test (2 V→6 V) to the cell were carried out using the facility of Enax Inc. No smoke and no fire of the cell during the experiment were observed under air atmosphere at a room temperature, although some extent of swelling was observed in the overcharge test. The present SPE containing Al-PEG and DMTG also did not have any fire even if ignition was tried by a torch. Thus, we believe that the nonflammable property in the present cell is maintained even at 120 °C. The DSC experiment also supports the behavior (Fig. 2).

It is desirable that the development of the large-scale lithium ion batteries by accumulating the single cell in the present study in the near future.

Conclusions

All-solid polymer electrolyte with nonflammable property was prepared from monomer mixture which contains two matrix components, PME400 and PDE600, and two plasticizers, Al-PEG with n=9 and DMTG with n=3, and dissolved lithium salt LiTFSI. Radical polymerization of the monomer was carried out by heating at 120 °C. The suitable polymerization temperature was estimated from the data of DSC. The ionic conductivity of the polymer electrolyte, SPE, was measured by making use of AC impedance techniques, and a rather higher value of 10^{-3} S cm^{-1}, which suggests the possibility of practical use, was observed at 60 °C. CV measurement of the SPE showed right voltage window between 4.0 and 3.0 V vs. Li^+/Li. The present SPE had some of undesirable sub-reaction with usual graphite-anode. Therefore, the LTO anode and the LFP cathode were selected for constructing a new single cell. Nonflammable LTO|SPE|LFP cell was laminated, and the charge/discharge properties of the cell were examined at a room temperature and 50 °C. Since sufficient cycle performance was obtained, the development of large-scale lithium ion batteries would be desirable by accumulating present single cell in the near future.

Acknowledgments We thank the Matching Fund Program from the New Energy and Industrial Technology Development Organization (NEDO) of Japan (Project ID: 81063) for the financial support. Drs. M. Nakayama and S. Kuroki kindly measured PGStE-NMR spectroscopy in Tokyo Institute of Technology and gave useful comments and discussion. Dr. H. Miyashiro also kindly gave the heat flow data of the LFP electrode.

References

1. Inaguma Y, Chen I, Itoh M, Uchida T, Ikuta H, Wakihara M (1993) Solid State Commun 86:689–693
2. Kannno R, Maruyama M (2001) J Electrochem Soc 148:A742–A746
3. Hayashi A, Minami K, Mizuno F, Tatsumisago M (2008) J Mater Sci 43:1885–1889
4. Kamaya N, Homma K, Yamakawa Y, Hirayama M, Kanno R, Yonemura M, Kamiyama T, Kato Y, Hama S, Kawamoto K, Mitsui A (2011) Nature Mater Advance online publication, 1–5 (published online: 31 July 2011)

5. Fergus JW (2010) J Power Sources 195:4554
6. Bideau JL, Ducros J-B, Soudan P, Guyomard D (2011) Adv Func Mater 20:1–6
7. Fenton DE, Parker JM, Wright PV (1973) Polymer 14:589
8. Armand MB, Chabagno JM, Duclot MJ (1979) Fast ion transport in solids. In: Vashista P, Mundy JN, Shenoy GK (eds.) Elsevier, Amsterdam
9. MacCallum JR, Vincent CA (1987) Polymer Electrolyte Review 1. Elsevier, London
10. Armand MB, Gorecki W, Andreani R (1990) 2nd International Symposium on Polymer Electrolytes. In: Scrosati B (eds.), Elsevier, London, p21
11. Kato Y, Yokoyama S, Ikuta H, Uchimoto Y, Wakihara M (2001) Electrochem Commun 3:128–130
12. Kato Y, Hasumi K, Yokoyama S, Yabe T, Ikuta H, Uchimoto Y, Wakihara M (2002) Solid State Ionics 150:355
13. Kato Y, Yokoyama S, Yabe T, Ikuta H, Uchimoto Y, Wakihara M (2004) Electrochim Acta 50:281
14. Masuda Y, Seki M, Nakayama M, Wakihara M, Mita H (2006) Solid State Ionics 177:843–846
15. Wakihara M, Nakayama M, Kato Y (2009) Lithium ion rechargeable batteries. In: Ozawa K (eds.) Wiley-VCH, Weinheim, Chap. 9, p218
16. Kaneko F, Wada S, Nakayama M, Wakihara M, Koki J, Kuroki S (2009) Adv Func Mater 19:918–925
17. Kaneko F, Wada S, Nakayama M, Wakihara M, Kuroki S (2009) ChemPhysChem 10:1911–1915
18. Padihi AK, Najundaswamy KS, Goodenough JB (1997) J Electrochem Soc 144:1188–1194
19. Huang H, Yin S-C, Nazar LF (2001) Electrochem Solid-State Lett 4:A170
20. Morgan D, Van der Ven A, Ceder G (2004) Electrochem Solid-State Lett 7:A30
21. Yamada A, Koizumi H, Nishimura S, Sonoyama N, Kanno R, Nakamura T, Kobayashi Y (2006) Nat Mater 5:357
22. Sommerfield A (1956) Thermodynamic and statistical mechanics. Lectures on Theoretical Physics Academic, New York
23. Hong JS, Maleki H, Al Hallaj S, Redey L, Selman JR (1998) J Electrochem Soc 145:1489
24. Miyashiro H, (2006) Doctoral thesis, Tokyo Institute of Technology
25. Hahn EL (1950) Phys Rv 80:580–594
26. Tabata S, Hirakimoto T, Nishiura M, Watanabe M (2003) Electrochim Acta 48:2105–2112
27. Colbow KM, Dahn JR, Haering RR (1989) J Power Source 26:397
28. Ferg E, Gummow RJ, de Kock A, Thackeray AA (1994) J Electrochem Soc 141:L147
29. Ohzuku T, Ueda A (1994) Solid State Ionics 69:201
30. Scharner S, Weppner W, Schmid-Beurmann PJ (1999) Electrochem Soc 146:857
31. Ariyoshi K, Yamato R, Ohzuku T (2005) Electrochim Acta 51:1125–1129
32. Bakenov Z, Nakayama M, Wakihara M (2007) Electrochem Solid-State Lett 10:A208–A211
33. Krause L, Lammana W, Summerfield J, Engle M, Korba G, Loch R, Atanasoski R (1997) J Power Sources 68:320–325
34. Nakayama M, Wada S, Kuroki S, Nogami M (2009) Energy Environ Sci 3:1995–2002